Electronic Supplementary Information for

Monitoring Single Au_{38} Nanocluster Reactions via Electrochemiluminescence

Mahdi Hesari,[a] Hui Ma,*[b] Zhifeng Ding*[a]

[a]Department of Chemistry, The University of Western Ontario, London, Ontario N6A 5B7, Canada.

[b]State Key Laboratory of Analytical Chemistry for Life Science, School of Chemistry and Chemical Engineering, Nanjing University, Nanjing 210023, P.R. China.

*Corresponding authors:

Email: zfding@uwo.ca ; mahui@nju.edu.cn

Table of Contents

1. Materials

1.1. Chemicals

Hydrogen tetrachloroaurate trihydrate (Aldrich, 99.9%), sodium borohydride (Aldrich, 99%), methanol (Caledon, 99.8%), phenylethanethiol (Aldrich, 98%), trans-2-[3-(4-tert- butylphenyl)-2-methyl-2-propenylidene]-malononitrile (DCTB, Aldrich 98%), ethanol (Caledon, 99.8%), ferrocenemethanol (Aldrich, 97%), ferrocene (Aldrich, 98%) and acetonitrile (Caledon) were used as received. Tetra-n-butylammonium perchlorate was provided by Fluka (99%) and kept in dry condition before use. Anhydrous acetonitrile (99.8%) and anhydrous benzene (99.8%), tri-*n*-propylamine (Aldrich, 98%) were purchased from Aldrich.

2. Synthesis of Au_{38} nanocluster

$Au_{38}(SC_2H_4Ph)_{24}$ nanoclusters were prepared according to size focusing synthetic protocol.[1] $HAuCl_4.3H_2O$ (196.6 mg, 0.5 mmol) and glutathione (614.0 mg, 2.0 mmol) were mixed in 20 mL of acetone at room temperature. The mixture was stirred for 20 min and the resulted yellowish cloudy suspension was then cooled to 0°C for 20 min. $NaBH_4$ (5 mmol, 189.0 mg) dissolved in 6 mL of cold deionized water and rapidly added to the suspension under vigorous stirring. At this stage, the color of the solution immediately turned black, indicating the formation of $Au_n(SG)_m$ intermediate that were found to precipitate out and stick to the inner wall of the reaction container. After decanting the supernatant the obtained $Au_n(SG)_m$ was re–dispersed in 6 mL of nanopure water. Next, a mixture of 0.6 mL of ethanol, 2 mL of toluene, and 2.5 mL of phenylethenethiol was added. The solution was refluxed at 80°C for overnight. The UV-visible spectrum of the crude product was measured after 18h. Then, the reaction was cooled down to room temperature and the product was extracted with dichloromethane and collected.

The pure Au_{38} nanoclusters was obtained after washing the oily crude product thoroughly with methanol to remove excess of the thiol. The nanocluster were effectively characterized using UV-Visible-NIR (**Fig. S1**) and photoluminescence (PL)(**Fig. S2**) spectroscopy and proton NMR spectroscopy (**Fig. S3**) along with matrix assisted laser desorption (MALDI) mass spectrometry (**Fig. S4**), which agree very well with those from the Jin group[2, 3], Liljeroth and Quinn *et al.*[4] and our lab.[1] to confirm the Au_{38} nanocluster synthesis.

3. $Au_{38}(SC_2H_4Ph)_{24}^0$ nanocluster characterization

A 0.05 mM $Au_{38}(SC_2H_4Ph)_{24}^0$ in dichloromethane was used to collect UV-Visible-NIR absorption spectra using a Carry 5000 instrument. The obtained spectrum reavled four electronic transitions as shown in **Fig. S1**. The same sample was illuminted with a 532-nm solid state laser to collect the PL spectrum (**Fig. S2**) using a iDus CCD camera (Model DU401-BR-DD-352) and a Acton 2300i spectrograph with an emission peak wavelength at 930 nm. ^{1}HNMR spectrum of $Au_{38}(SC_2H_4Ph)_{24}^0$ sample was collected in $CDCl_3$ and two distict are corresponding to aliphatic (2.70–4.16 ppm) and aromatic protons (6.88–7.32

ppm) of the protecting ligands were identified (**Fig. S3**). Moreover, An AB Applied Biosystem mass spectrometer (4700 Proteomics Analyzer) was employed to obtain MALDI-TOF spectra. The sample was prepared by mixing 0.2:1000 analyte to matrix ratio. Then, 7 μL of the mixture was casted on the target plate and air-dried (**Fig. S4**). The parent peak at 10778.06 Da represents the molecular mass of of $Au_{38}(SC_2H_4Ph)_{24}{}^0$.

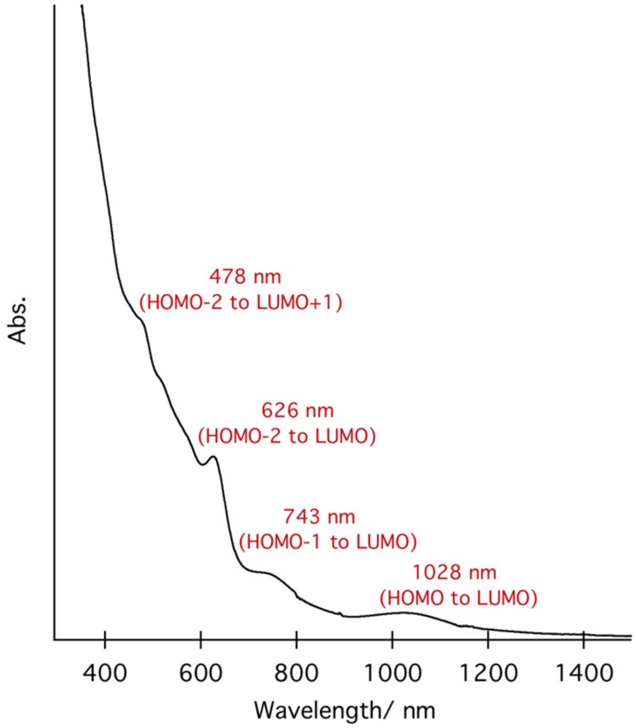

Fig. S1. UV-Visible-NIR absorption spectrum of $Au_{38}(SC_2H_4Ph)_{24}{}^0$ in dichloromethane.

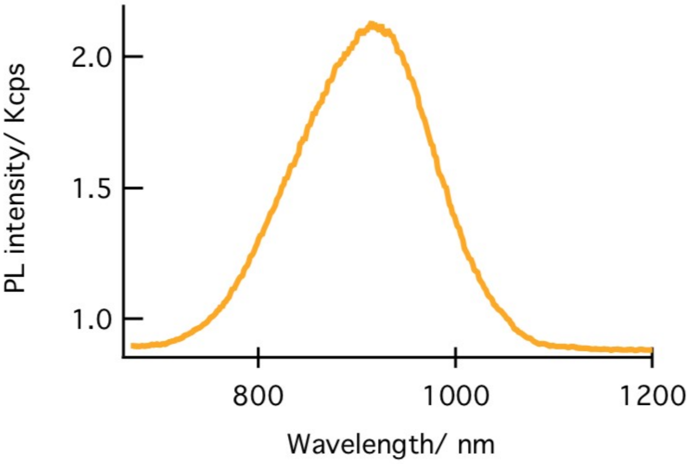

Fig. S2. Photoluminescence spectrum of $Au_{38}(SC_2H_4Ph)_{24}^0$ in dichloromethane. A 532-nm laser was used to excite a 0.05 mM Au_{38} solution.

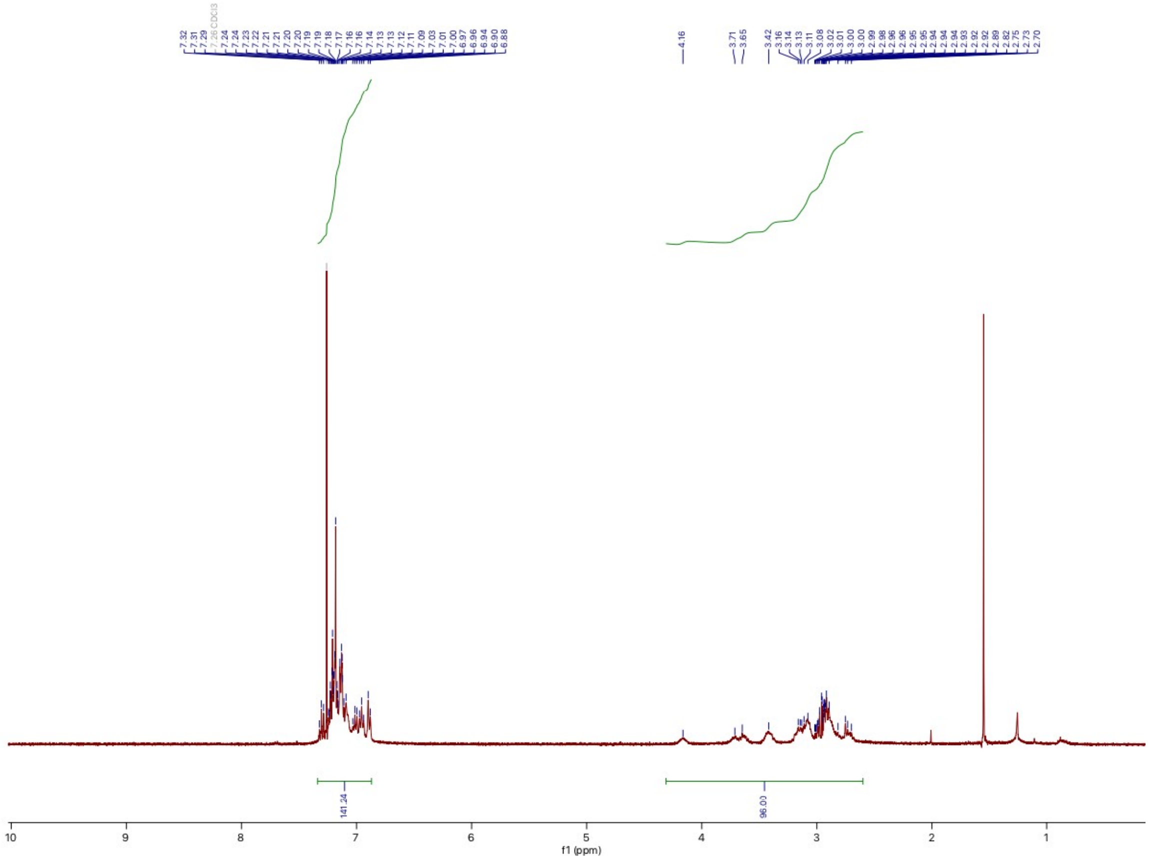

Fig. S3. ^{1}HNMR spectrum of $Au_{38}(SC_2H_4Ph)_{24}^0$ in $CHCl_3$.

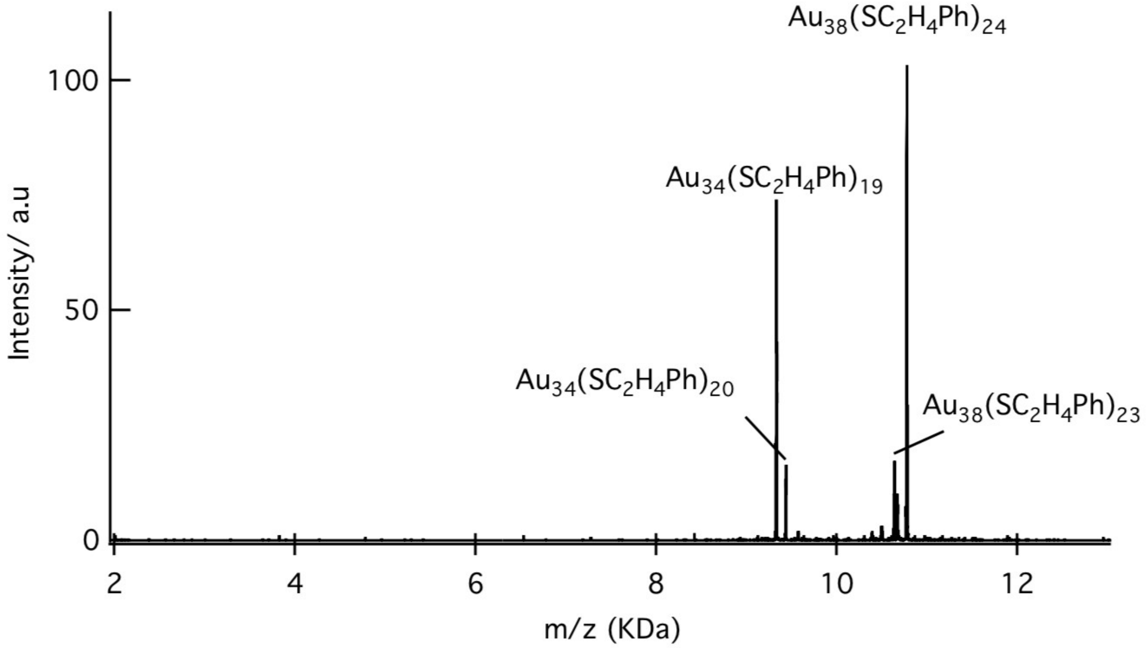

Fig. S4. Matrix assisted laser desorption mass spectrometry of $Au_{38}(SC_2H_4Ph)_{24}{}^0$.

4. Electrochemiluminescnce measurements

The conventional electrochemistry and ECL of the Au_{38} nanocluster were conducted using a 10 μm or 2 mm diameter Pt disc inlaid in a glass sheath as the working electrode (WE), a coiled Pt wire as the counter electrode (CE), and a coiled Pt wire as the quasi-reference electrode (QRE). The electrochemical potential window was calibrated using ferrocence as the internal standard. The redox potential of the ferrocene/ferrocenium (Fc/Fc^+) couple was taken as 0.424 V vs. SCE.[1] A solution containing approximately of Au_{38} clusters, 0.1 M TBAP as the supporting electrolyte and 1.5 mL anhydrous acetonitrile and anhydrous benzene was added to the electrochemical cell with a flat Pyrex window at the bottom for detection of generated ECL, which was assembled in a glovebox. TPrA were also added to the electrochemical cell under Ar (99.999%) blanket to prevent oxygen penetration the sample solution.

The cyclic voltammetry was performed on a CHI 610A electrochemical analyzer (CH Instruments, Austin, TX). The ECL–potential curves and ECL–time transients were obtained using the CHI 610A coupled with a photomultiplier tube (PMT, R928, Hamamatsu, Japan) held at -750 V by a high voltage power supply. The ECL intensity was collected by the PMT under the flat Pyrex window at the bottom of the cell was measured as a photocurrent, and transformed to a voltage signal, using a picoammeter/voltage source (Keithley 6487, Cleveland, OH). The potential, current signals from the electrochemical workstation, and the ECL signal from the picoammeter were sent simultaneously through a DAQ board (DAQ 6052E, National Instruments, Austin, TX) to a computer. The data acquisition system was controlled from a home-written LabVIEW program. The photosensitivity on the picoammeter was set manually in order to avoid the signal saturation.

The ECL spectra were recorded using the Andor Technology program. Since the ECL is in NIR region, ECL spectroscopy was conducted on an Acton 2300i spectrograph with two gratings (50 *l*/mm blazed at 600 nm and 300 *l*/mm blazed at 700 nm) and an Andor iDUS CCD camera (Model DU401-BR-DD-352) that cooled down to -70°C. The set of the spectrograph and camera was calibrated using a mercury-argon lamp each time. The accumulation spectra were recorded during 30 min holding a desired potential value.

4.1 ECL-voltage curves at 2-mm electrodes

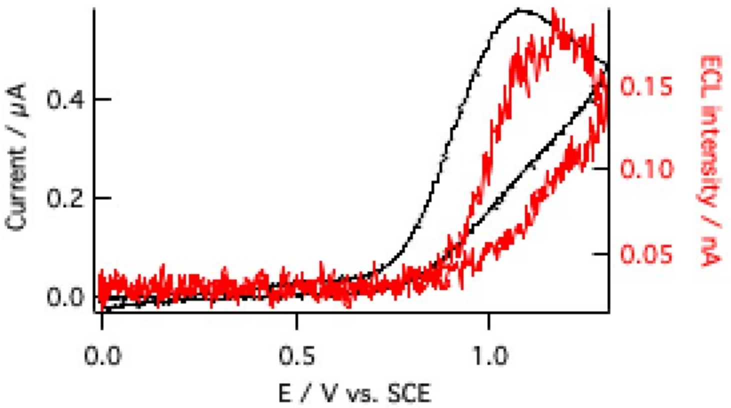

Fig. S5. ECL–voltage curve of 10 µM Au_{38} nanoclusters in 1:1 acetonitrile/benzene containing 0.1 M $TBAPF_6$, in the presence of TPrA using a 2-mm disk electrode at 100 mVs^{-1} scan rate.

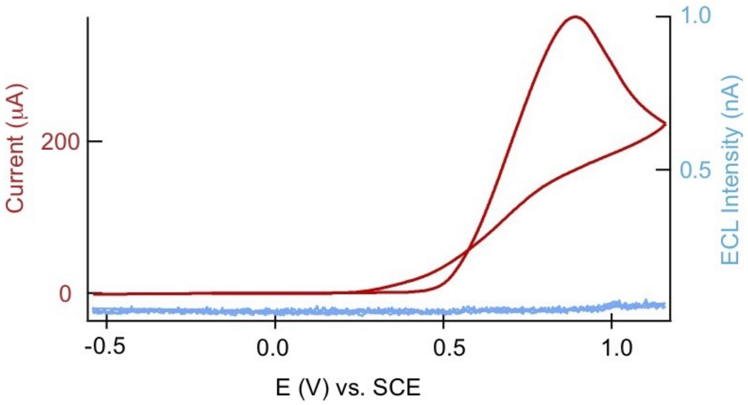

Fig. S6. ECL–voltage curve of 20 mM TPrA in 1:1 acetonitrile/benzene containing 0.1 M $TBAPF_6$, using 2-mm diameter Pt disk electrode at 100 mVs^{-1} scan rate.

4.2 Ultramicroelectrode preparation

A 10 μm Pt wire (99.999%) was sealed in a borosilicate glass tube (OD:1.0 mm, ID:0.5 mm) using a heating puller (Narishige International USA, Inc., model PC-100-CA). Then, the UME was polished using polishing pads (3, 1, and 0.3 micron). Final polishing performed with 0.3 micron alumina pad to produce the smoothest electrode surface and a cyclic voltammogram was run in a 0.9 mM ferrocenemethanol in phosphate buffer pH=7 at 20 mVs^{-1} (**Fig. S7**).

4.3 Cyclic voltammogram at Pt UME

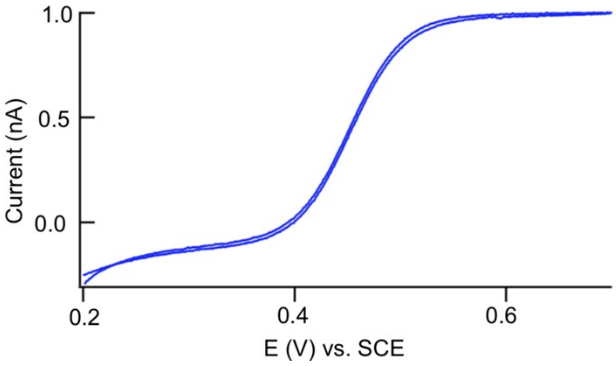

Fig. S7. Cyclic voltammogram of Pt UME in 0.9 mM ferrocene methanol phosphate buffer pH=7 at 20 mVs^{-1}.

4.4 Detailed single Au_{38} nanocluster reaction mechanisms

Hesari et. al., previously detailed the ECL emission mechanisms of Au_{38} nanoclusters.[1] In the course of a single reaction the co-reactant, TPrA, is oxidized to its radical cation (eqn (S1)), following losing a proton (eqn (S2)). At a very close potential, Au_{38} is also oxidized to Au_{38}^{3+}, which is highly reactive (eqn (S3)). Thus, an in-situ reaction between nanocluster and TPrA results in the generation of an excited state (Au_{38}^{2+*}, eqn (S4)). The relaxation process of Au_{38}^{2+*} to Au_{38}^{2+} gives a NIR-ECL emission at 930 nm (eqn (S5)).

$$TPrA \rightarrow TPrA^{\cdot +} + e^{-} \tag{S1}$$
$$TPrA^{\cdot +} \rightarrow TPrA^{\cdot} + H^{+} \tag{S2}$$
$$Au_{38}^{0} \rightarrow Au_{38}^{3+} + 3\,e^{-} \tag{S3}$$
$$Au_{38}^{3+} + TPrA^{\cdot} \rightarrow Au_{38}^{2+*} + Pr_2N^{+} = CHCH_2CH_3 \tag{S4}$$
$$Au_{38}^{2+*} \rightarrow Au_{38}^{2+} + hv \tag{S5}$$

5. ECL–time transient analysis

Single–nanocluster ECL–time trajectories were processed by home–written MATLAB code including ECL signals location as well as evaluations of amplitude for accurate analysis of individual photoelectrochemical signals that is adopted from Ref. 2. For each recognized ECL signal, a 2nd order differential based calibration (DBC) method was introduced to correct the over-coverage.[5]

Location of photocurrent signals. In order to achieve rapid data analysis, it is necessary to decrease the processing time on the intervals between two current signals. Therefore, we roughly locate the ECL intensity represented by photocurrent in nA as the first step in our data process. To minimize the influence of baseline drifting, a local baseline was estimated based on moving window averaging. The adjustable window width ω is related to the noise level. The local threshold (u_j) could be defined by subtracting a constant threshold (u_0) from the local baseline eqn (S6).

$$u_i = \frac{1}{\omega} \sum_{k=j-\omega}^{j} I_k - u_0 \tag{S6}$$

where I_k is value of the photocurrent at data point k. A program scans throughout the whole current trace to search and mark the data points whose current is lower than the corresponding local threshold (ignore the boundary effect).

Current amplitude of the photocurrent signals. Conventionally, the amplitude of photocurrent signals (I_c) is evaluated by subtracting the minimum (or average of plateau) from the baseline. However, the rise time (T_r) of low-pass filter deviates the current signals to reach their real minimum or plateau. Usually, photocurrent signals with t_d less than $2T_r$ are seriously attenuated. The T_r of a filter could be estimated by eqn (S7),

$$T_r = 0.3321/f_c \tag{S7}$$

where f_c is the cut-off frequency of filter. For a 3 kHz low-pass filter, the value of $2T_r$ is approximately 0.22 ms. The low-pass filter removes the short-term fluctuations such as flicker noise while deforms the blockade shape. Nevertheless, the area of a current signal is hardly affected by a low-pass filter. In other words, the integrated area is more suitable than minimum (or plateau) to act as the criterion for the measurement of current amplitude, particularly for current signals with t_d less than $2T_r$. As inspired by the nature of filter, a novel integration method is used as the next step in our data process to accurately evaluate current amplitude. Because of the low-pass filter, the current signal is modified seriously and drops slowly without reaching the minimum of square wave. Therefore, the unmodified current amplitude (I_c) could be calculated via eqn (S8). Considering the recorded data point is discrete, eqn (S8) could be transformed to eqn (S9).

$$I_c t_d = \int_{t_{start}}^{t_{end}} (I_{base} - I(t))dt \tag{S8}$$

$$I_c t_d = \frac{1}{f_s} \sum_{k=P_{s2}}^{P_{e2}} (I_{base} - I_k) \tag{S9}$$

where t_d is the duration time of the square wave, f_s is the sampling frequency of analogy-to-digital convertor, I_{base} is the baseline current, I_k is the current value at data point k.

6. Photomultiplier tube (PMT) performance

6.1. Basic light-to-photocurrent conversion in a PMT

A typical photomultiplier tube (i.e., PMT) has a transparent glass body (e.g., silica, saphier, MgF_2 crystal, Uv-glass, Borosilicate) with different transmission windows. Inside a PMT three main components consist of; photocathode, dynodes, and photoanode. Basically, an incident light (i.e., generated light due to relaxation of a luminophore) hits the photocathode and produces first generation of photoelectron current (cathode current). Next, this photoelectron reaches to an electron multiplier that is dynode which can be made of variety of materials such as magnesium oxide (MgO), beryllium oxide (BeO), gallium phosphide (GaP). These materials can generate secondary electrons that due to the vacuum and applied voltage (between anode and cathode) results in amplification of photocurrent and enhance the detection signal. Finally, the accelerated photoelectrons his photoanode that collects all the secondary electrons and transfer them to the external electrical circuit.[6] This process is illustrated in **Fig. S8**.

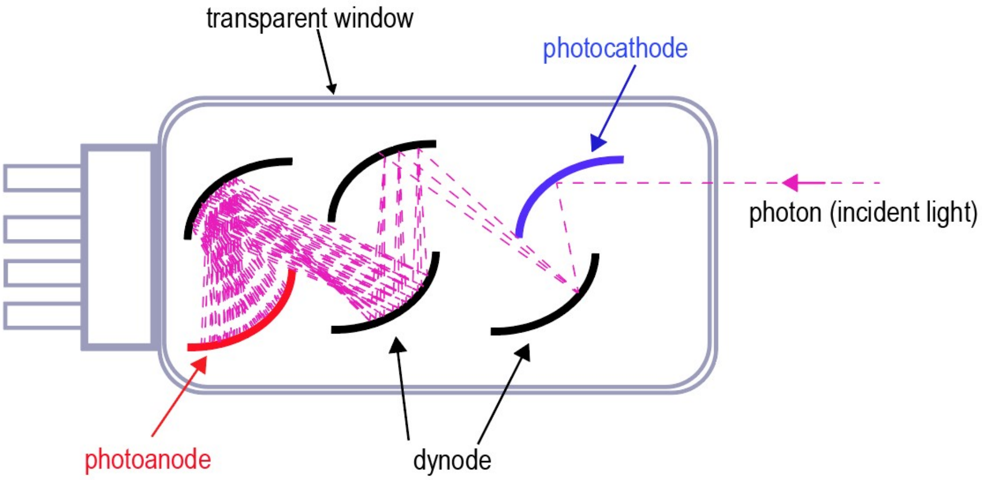

Fig. S8. Schematic of a photomultiplier tube light-to-photocurrent conversion.

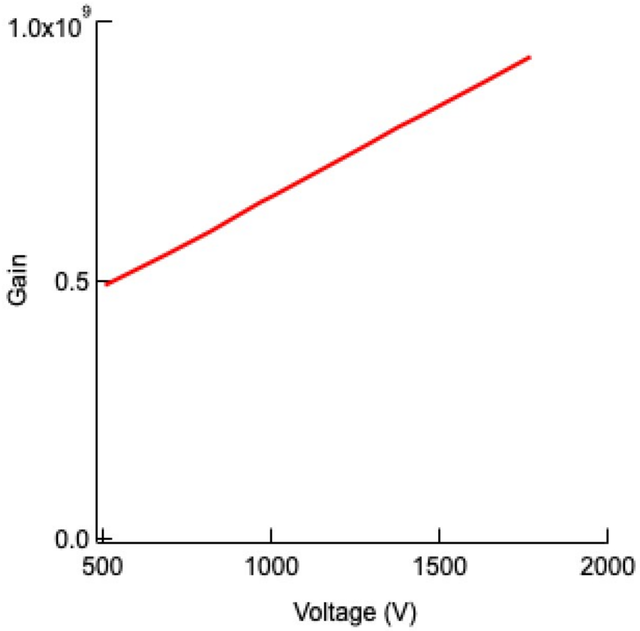

Fig. S9. PMT gain versus applied voltage for R928 model.

6.2. Response curve of PMT and quantum efficiency spectra of CCD camera

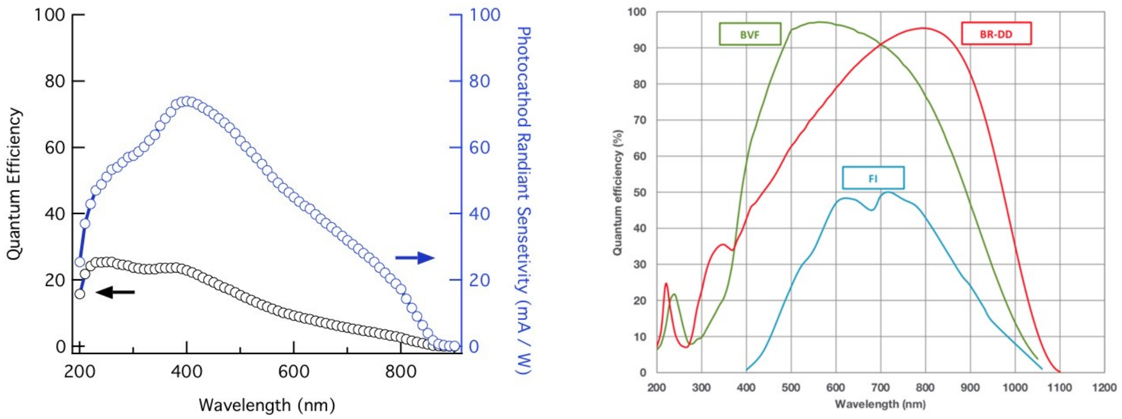

Fig. S10. The response curve of Hamamatsu R928 PMT (left) and quantum efficiency spectra of Andor CCD camera (right).

7. Extra ECL transients and spectra

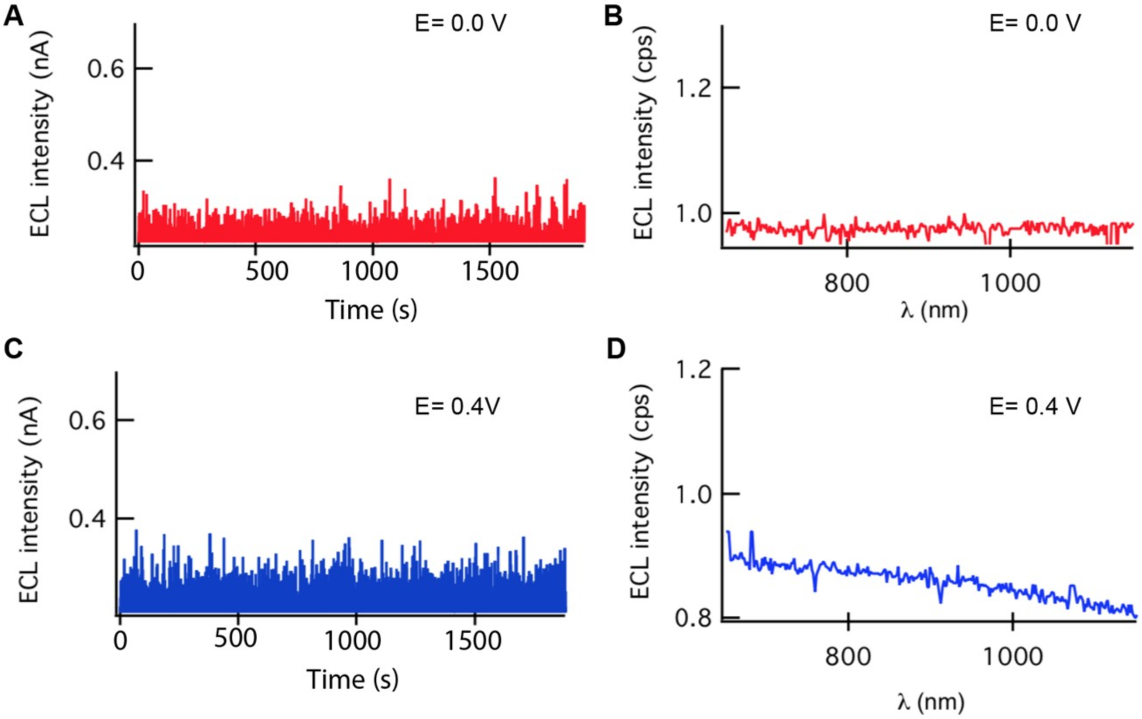

Fig. S11. Background ECL-time transients and spectra. ECL-time transient (**A**) and accumulated ECL spectrum (**B**) at 0.0 V vs. SCE. ECL-time transient (**C**) and accumulated ECL spectrum (**D**) at E= 0.4 V vs. SCE.

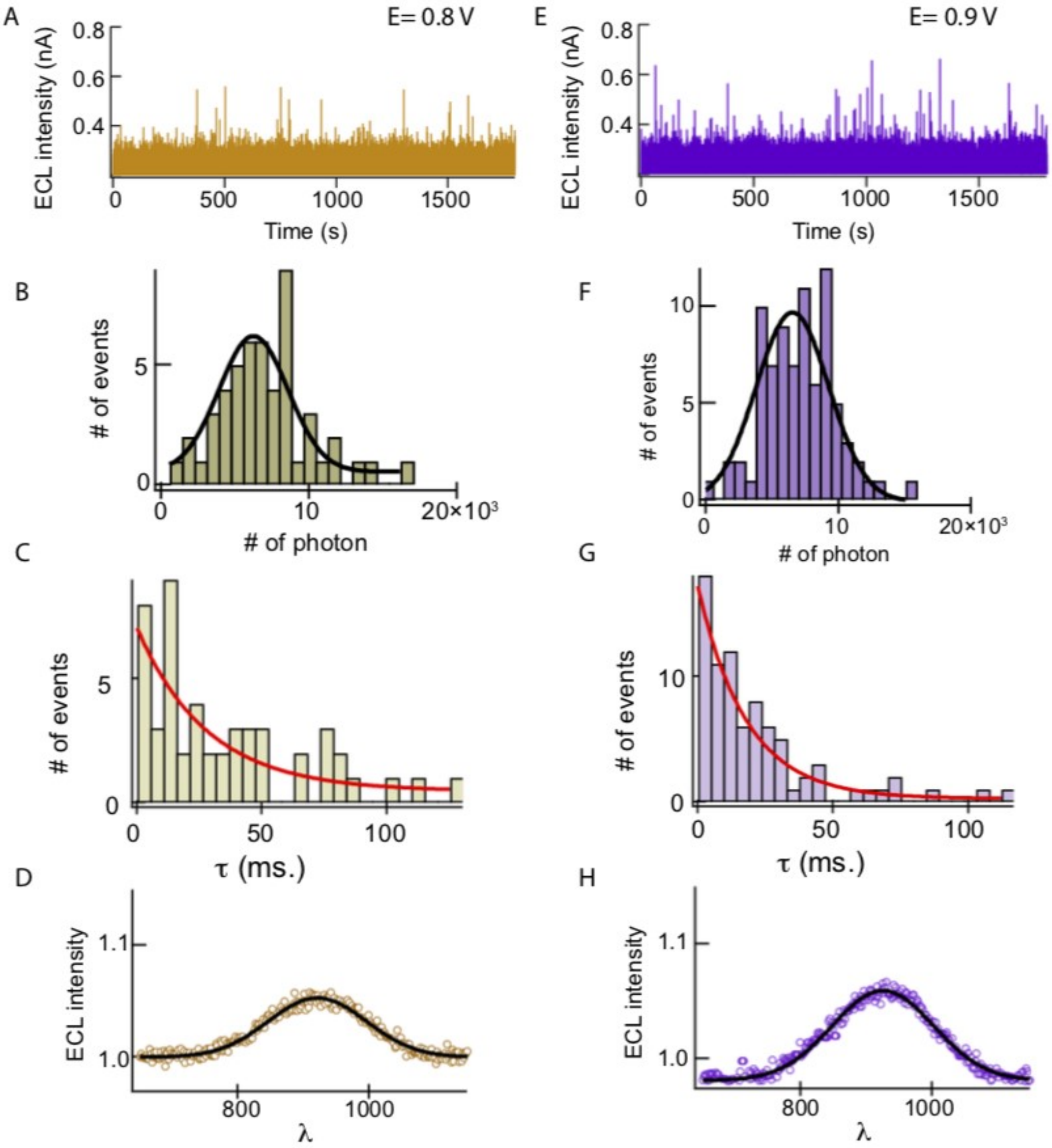

Fig. S12. ECL versus time trajectory analyses. (**A**) ECL vs. time transient at 0.8 V vs. SCE. (**B**) histogram of counted number of photons obtained from (**A**), (**C**) histogram of temporal sequence of light generation reactions (τ) from transient at (**A**), (**D**) Accumulated ECL spectrum collected for 30 min. (**E-H**) represent the same analyses at E= 0.9 V vs. SCE.

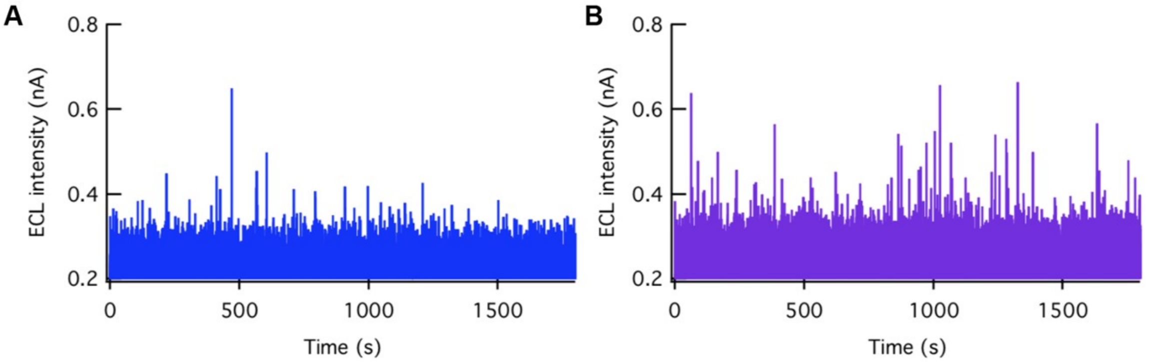

Fig. S13. ECL versus time trajectory analyses. (**A**) [Au_{38}^{0}]= 5 μM, (**B**) [Au_{38}^{0}]=20 μM in the presence of 20 mM TPrA in benzene/ acetonitrile (1:1) contain 0.1 M $TBAPF_6$ at E=1.1 V vs. SCE.

8. Cross-correlation investigation of ECL intensity and spikes time-delay (τ)

Cross-correlation (ρ) is an indication of relationships between two parameters (e.g., spike intensity and τ). By definition: when $\rho>1$ it means there is a positive correlation within two examined variables. However if $\rho<1$, there is no correlation between those variables.[7]

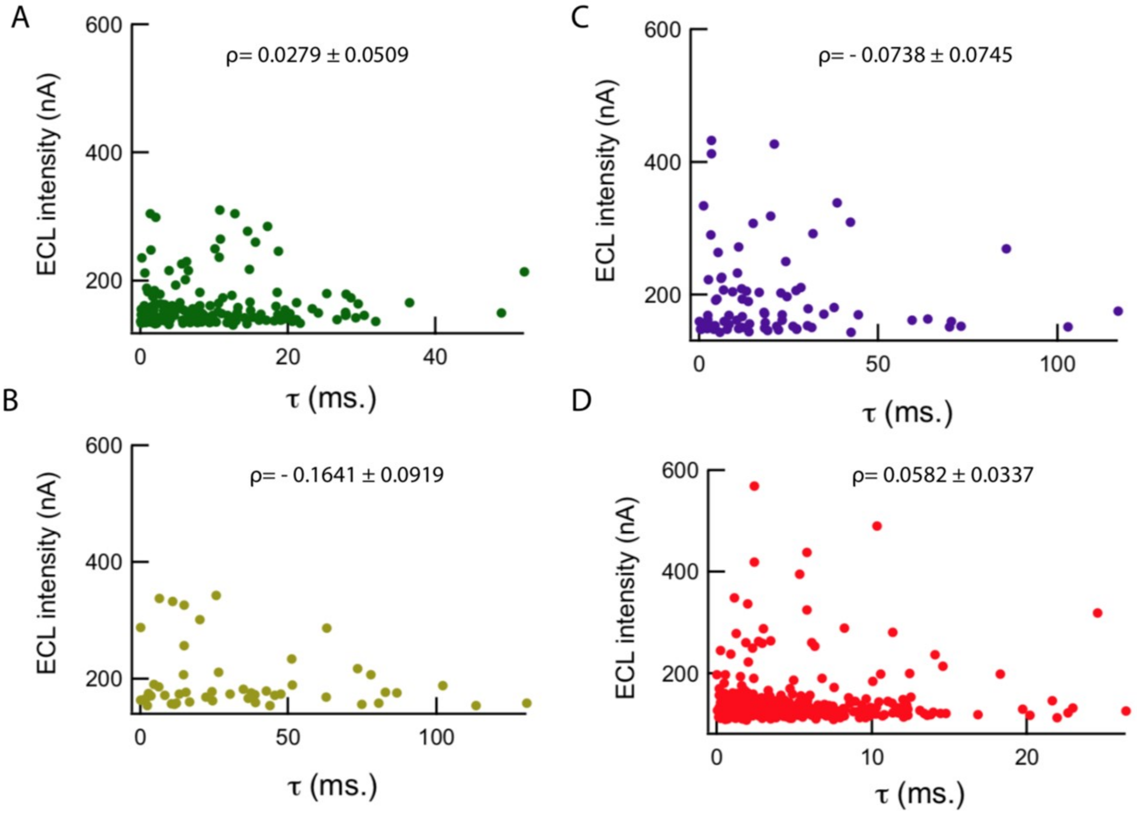

Fig. S14. Cross-correlation plots of spike ECL intensity versus reaction time interval between reaction sequences at different potentials as (**A**) E= 0.7, (**B**) E=0.8, (**C**) E=0.9, and (**D**) E=1.0 V vs. SCE.

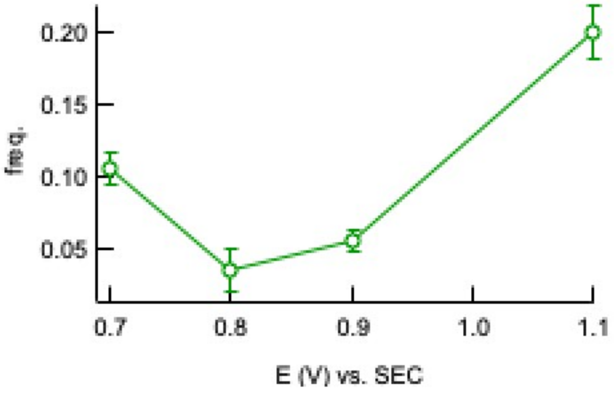

Fig. S15. Frequency of averaged single reaction at different potentials.

References:

1 M. Hesari, M. S. Workentin and Z. Ding, *ACS Nano*, 2014, **8**, 8543-8553.
2 H. Qian, Y. Zhu and R. Jin, *ACS Nano*, 2009, **3**, 3795-3803.
3 H. Qian, M. Zhu, C. Gayathri, R. R. Gil and R. Jin, *ACS Nano*, 2011, **5**, 8935-8942.
4 O. Toikkanen, V. Ruiz, G. Rönnholm, N. Kalkkinen, P. Liljeroth and B. M. Quinn, *J. Am. Chem. Soc.*, 2008, **130**, 11049-11055.
5 Z. Gu, Y.-L. Ying, C. Cao, P. He and Y.-T. Long, *Anal. Chem.*, 2015, **87**, 907-913.
6 Hamamatsu, in *Photomultiplier tubes; basics abd applications*, Hamamatsu Photonics K.K., Third edition edn., 2007.
7 J. S. Bendat and A. G. Piersol, *Random Data: Analysis and Measurement Procedures*, John Wiley & Sons, Inc., 4th edn., 2010.